

## Activation barriers to strain relaxation in lattice-mismatched epitaxy

R. Hull, J. C. Bean, D. J. Werder, and R. E. Leibenguth

*AT&T Bell Laboratories, 600 Mountain Avenue, Murray Hill, New Jersey 07974*

(Received 14 March 1989)

We study the activation barriers to strain relaxation in metastable  $\text{Ge}_{0.25}\text{Si}_{0.75}/\text{Si}(100)$  films by *in situ* annealing in a transmission electron microscope, observing in real time the dynamic relaxation events of misfit-dislocation nucleation, propagation, and interaction as a function of the sample annealing temperature. Activation energies for misfit-dislocation nucleation and propagation are obtained, and it is firmly established that both these processes and dislocation interactions inhibit strain relaxation in  $\text{Ge}_x\text{Si}_{1-x}/\text{Si}$  epitaxy.

Strained-layer heteroepitaxial growth of semiconductor materials with different lattice constants has opened a wide new field of study of the structural and electronic properties of these materials.<sup>1,2</sup> It has long been recognized that there will exist a characteristic thickness  $h_c$  at which it will be energetically favorable for misfit dislocations to relax a tetragonally distorted epilayer. While early models of this "critical thickness" phenomenon<sup>3,4</sup> predicted  $h_c$  based upon equilibrium considerations, it has been found experimentally that in many strained-layer systems growth at moderate substrate temperatures (e.g., in the  $\text{GeSi}/\text{Si}$  system<sup>2</sup>) enabled experimental values of  $h_c$  to significantly exceed equilibrium predictions. This was shown experimentally<sup>5,6</sup> to be due to the fact that  $\text{Ge}_x\text{Si}_{1-x}/\text{Si}$  films could be grown in a metastable state, presumably due to the activation barriers associated with misfit-dislocation formation and/or motion. A recent model of critical thickness phenomena,<sup>7,8</sup> provided good agreement with experimental data by associating the motion of dislocations with the excess stress in the films. Dislocation formation is assumed to be via a vanishingly small activation energy multiplication or source process, and the activation energy for dislocation propagation is obtained from previous measurements<sup>9</sup> of dislocation glide in plastically deformed Ge and Si (1.6 and 2.2 eV, respectively). However, to date, no direct real-time experimental observations of dislocation motion and interactions in thin strained-layer epitaxial semiconductor films have been reported. In this paper, we report such measurements and show that both the activation energies for dislocation formation and propagation are significant. In addition we show how dislocation interactions critically limit the rate at which elastic strain relaxes.

The essential experimental geometry for these experiments has been described previously.<sup>10</sup> In brief, thin-foil  $\text{Ge}_{0.25}\text{Si}_{0.75}/\text{Si}(100)$  samples are prepared via backside chemical etching in the plan view geometry for imaging in the transmission electron microscope (TEM). The  $\text{Ge}_{0.25}\text{Si}_{0.75}/\text{Si}(100)$  samples are grown by molecular-beam epitaxy (MBE) at a substrate temperature of 550°C, with epilayer thicknesses  $\sim 350$  Å, which is just below the experimentally determined critical thickness for this growth temperature.<sup>2</sup> The average misfit-dislocation sep-

aration in these as-grown samples, as determined from plan-view TEM, is of the order 5  $\mu\text{m}$ . This corresponds to relaxation of  $\sim 1\%$  of the elastic strain in a completely commensurate  $\text{Ge}_{0.25}\text{Si}_{0.75}$  epilayer. We then observe strain relaxation *in situ* in the electron microscope by heating the sample to temperatures  $\geq 550$ °C in a single-tilt holder. Sample temperatures are measured with a Pt/Rh thermocouple. The plan-view geometry of our experiment ensures that the  $\text{Ge}_x\text{Si}_{1-x}/\text{Si}$  interface is buried away from any free surfaces (as would not be the case for the cross-sectional geometry), and we are careful to record observations in regions of the sample which are both relatively thick, such that there is a significant thickness of substrate supporting the epilayer (the penetration depth of 200-kV electrons in Si is  $\sim 1$   $\mu\text{m}$ , making this requirement feasible for the samples studied here), and which are a significant distance (at least several  $\mu\text{m}$ ) from the thin-foil edge. The rigid substrate assumption is thus approximately valid for these experiments. Images are recorded on both photographic negatives (to record the number of misfit dislocations) and in real time using video imaging from a television camera located in the TEM final image plane (to view dynamic events such as dislocation velocities).

Figure 1 shows images of the misfit-dislocation network in a 350-Å  $\text{Ge}_{0.25}\text{Si}_{0.75}/\text{Si}(100)$  sample: (a) as grown, (b) after a 4-min anneal at 700°C, and (c) after a 4-min anneal at 900°C. An orthogonal mesh of  $\frac{1}{2}\langle 011 \rangle$  misfit dislocations is observed, the density increasing dramatically with annealing temperature. We observe that significant film relaxation occurs even at an annealing temperature of 550°C (the original sample growth temperature) showing that the initial film is grown in a highly metastable state. It is also found that the measured strain relaxation rates are highly sensitive to the local initial stress (i.e., composition and thickness) of the as-grown films.

By repeated experiments and analysis of real-time video imaging, we were also able to measure misfit-dislocation velocities in the temperature range 550–800°C (velocities at greater temperatures were too fast to measure within the time resolution afforded by individual video frames). The measured velocities are plot-

ted on an Arrhenius curve in Fig. 2. Note that the excess stress in the film as defined by Dodson and Tsao<sup>7,8</sup> does not change by more than  $\sim 10\%$  in these experiments. The effects of variation in this parameter on the dislocation velocity are thus not critical here. From Fig. 2, the measured activation energy for dislocation motion is  $1.1 \pm 0.2$  eV (the line of best fit shown in the figure is

determined via least-squares analysis with sample weighting assigned according to the inverse of the standard error in each measurement, while errors are conservatively estimated from the range of possible lines which may be drawn within the data error bars). This is considerably lower than the value of  $\sim 2.0$  eV which would be obtained by interpolation of the equivalent activation ener-

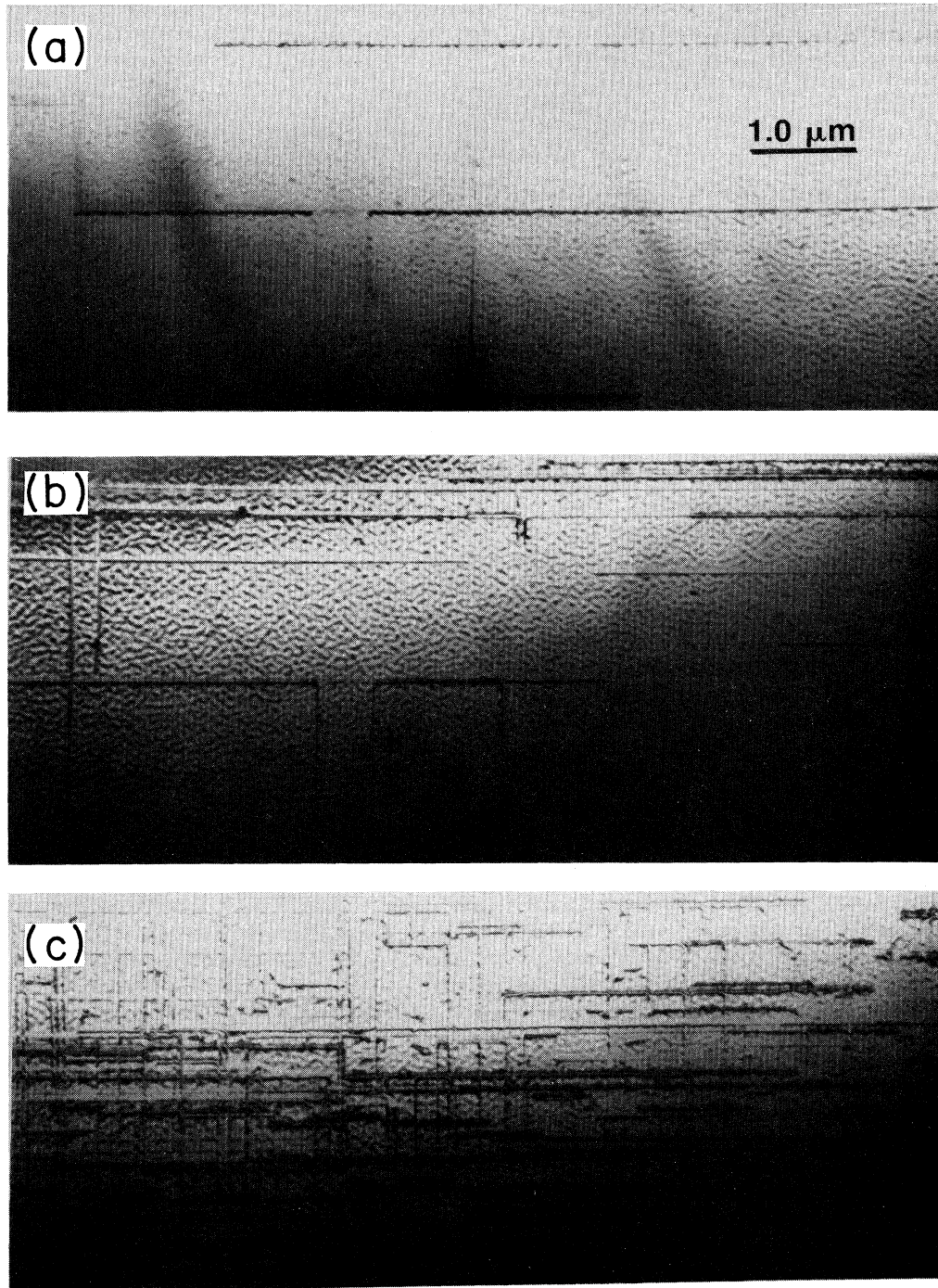


FIG. 1.  $\langle 022 \rangle$  plan-view TEM images of 350-Å  $\text{Ge}_{0.3}\text{Si}_{0.7}/\text{Si}(100)$  films: (a) as grown, and annealed for 4 min at (b) 700°C and (c) 900°C. Orthogonal arrays of  $\frac{1}{2}\langle 011 \rangle$  dislocations are observed.

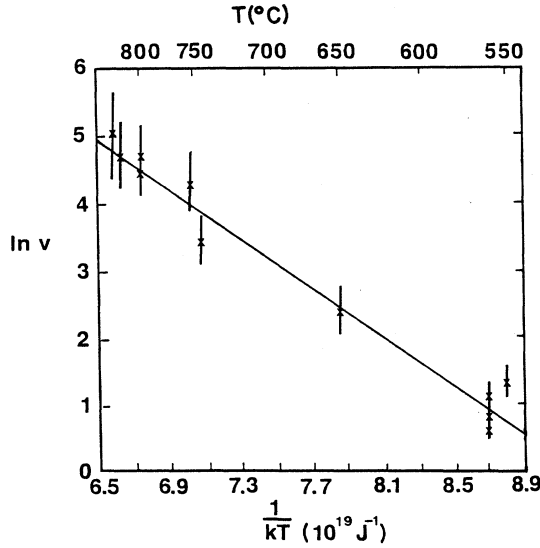


FIG. 2. Arrhenius plot of dislocation velocities in a 350-Å  $\text{Ge}_{0.25}\text{Si}_{0.75}/\text{Si}(100)$  film.

gies for bulk Ge and Si.<sup>9,11</sup>

To determine the effects of dislocation interactions on strain relaxation, we deduce a relationship between dislocation separation, dislocation length, and number of dislocations. Such a relationship is necessary for accurate determination of average dislocation length because of the limited field of view in the TEM images which would necessarily weight direct measurement of dislocation length towards shorter dislocations. Consider a wafer of diameter  $L$  and a measured average dislocation spacing  $p$ . Although the average dislocation length  $\bar{l}$  we measure is  $\ll L$ , the total length of misfit dislocation  $l_T$  is approximately equivalent to  $L/p$  dislocation lines running across the length of chords of the wafer a distance  $p$  apart (there will be two orthogonal sets of these chords);  $l_T$  will then be given by the number of dislocation lines ( $2L/p$ ) multiplied by the average chord length (this can be shown geometrically to be equal to  $2L/\pi$ )

$$l_T = \frac{4L^2}{p\pi}. \quad (1)$$

For  $\bar{l} \ll L$ , misfit dislocations must generally terminate either by deflecting from the interfacial  $\text{Ge}_x\text{Si}_{1-x}/\text{Si}$  plane to the wafer surface (a "threading dislocation") or by termination on another defect. The total number of dislocation terminations  $N_t$  may then be related to the total number of misfit dislocations  $N_l$  by the relation  $N_t \sim 2N_l$ . As  $N_l$  will be given by the total dislocation length  $l_T$  divided by the average length  $\bar{l}$ , the areal density of misfit-dislocation terminations  $n$  will be given by

$$\frac{n\pi L^2}{4} = \frac{2l_T}{\bar{l}}. \quad (2)$$

Substituting for  $l_T/L^2$  from Eq. (2) into Eq. (1) gives

$$\bar{l} = \frac{32}{p\pi^2 n}. \quad (3)$$

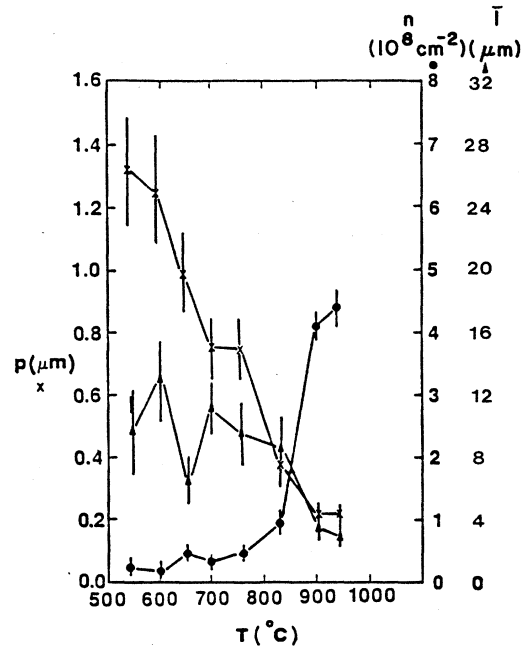


FIG. 3. Observed average dislocation separations  $p$  ( $\times$ ), observed areal dislocation densities,  $n$  ( $\bullet$ ), and calculated average dislocation lengths  $l$  ( $\blacktriangle$ ). These results are obtained for successive 4-min anneals at each of the temperatures for which experimental data are given. The film was 350-Å  $\text{Ge}_{0.25}\text{Si}_{0.75}/\text{Si}(100)$ .

We can thus determine  $\bar{l}$  in terms of  $p$  and  $n$  which we may measure from the electron micrographs. The variation of  $p$ ,  $\bar{l}$ , and  $n$  with respect to annealing temperature for consecutive 4-min anneals of a 350-Å-thick film is shown in Fig. 3. It is found that  $p$  decreases and  $n$  increases significantly with temperature, while  $\bar{l}$  remains relatively constant over most of the temperature range studied. This approximately constant value for  $\bar{l}$  does not imply a characteristic dislocation length of this value, rather as more and more dislocations are generated (and thus initially have very short length) as a function of temperature, more and more dislocations have to grow to lengths significantly greater than  $\bar{l}$  to keep the average value fixed. The fact that  $\bar{l}$  does not increase with time, however, is clear evidence that dislocation nucleation and/or multiplication as well as propagation are important in strain relaxation, and that dislocation interactions limit dislocation growth. Termination of misfit-dislocation lines at nodes with orthogonal dislocations is frequently observed, and by real-time imaging we observe that intersection events can either slow propagation or halt it. Finally, we note that as indeed  $\bar{l} \ll L$ , we can accurately determine the total number of dislocations from the measured areal density of dislocation termination  $n$  via Eq. (3).

In Fig. 4, we plot an Arrhenius plot of  $\ln N_t$  (proportional to areal dislocation density  $n$ ) versus inverse energy. These data, along with data from several equivalent experiments we have performed, produce an activation energy in the regime  $T < \sim 800^\circ\text{C}$  of  $0.3 \pm_{-0.1}^{0.2}$  eV. (We

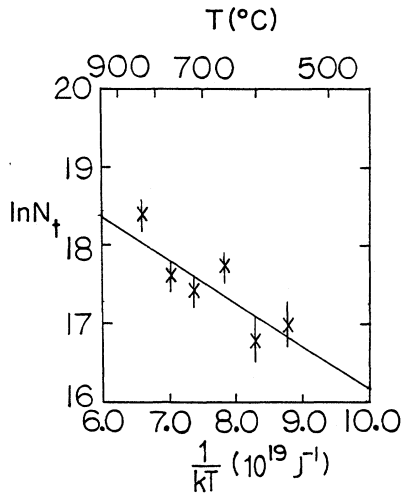


FIG. 4. Arrhenius plot of number of dislocations for a 350-Å  $\text{Ge}_{0.25}\text{Si}_{0.75}/\text{Si}(100)$  films. The film was annealed for 4 min at each of the temperatures for which the data are given.

note that for  $T > \sim 800^\circ\text{C}$  the activation energy appears to increase as suggested by the sudden increase in  $n$  in this range in Fig. 3.)

In conclusion, these *in situ* experiments have enabled us to directly observe dynamic events in strained-layer relaxation. The measured activation energy for dislocation propagation in these structures is significantly less than expected from measured values for glide in bulk Ge and Si. This discrepancy could be explained by assuming that the formation energy for kinks in these thin-film structures is significantly lowered by the presence of a free surface so close to the relaxing interface. The activation energy for glide, being the sum of kink formation and migration energies, is thus reduced. An alternative explanation, which in our opinion is more likely, is that as the annealing temperature and the dislocation density increase, the propagating dislocations have to cross more and more orthogonal dislocations in a given propagation

length. These intersection events are observed to impede propagation, which may be understood either by interdislocation forces or due to the acquisition of jogs (these are essentially kinks with a motion-retarding climb element). The low observed activation energy would then be a function of dislocation velocity reduction at high temperature rather than enhancement at low temperature. This model would thus argue that dislocation interactions, particularly in the later stages of strain relief, are of crucial importance. This concept, analogous to work hardening in metals, would have to be included in any predictive model of metastable strain relaxation. We discount strong effects of electron beam enhanced dislocation motion by noting that areas which are not irradiated by the electron beam relax at approximately the same rate as those which are irradiated. We also observe significant dislocation nucleation activation energies. Although we cannot rule out the presence of dislocation multiplication sources (we have never observed such mechanisms in real time, but have occasionally observed in static negatives configurations suggestive of the Hagen-Strunk multiplication mechanism<sup>12,13</sup> having operated), we believe that the primary mechanism for generating larger numbers of dislocations is by nucleation of new loops, as observed throughout the temperature range of our studies.

We believe that these experiments represent the first direct observations of dynamic relaxation events in metastable strained semiconductor layers. Such real-time observations enabling separate understanding of nucleation, propagation, and interaction events are shown to be of crucial importance in understanding strained-layer relaxation.

#### ACKNOWLEDGMENTS

We would like to acknowledge illuminating discussions with M. Grabow, J. M. Gibson, D. M. Maher, and R. People of AT&T Bell Laboratories, B. W. Dodson, I. Fritz, and J. Tsao of Sandia National Laboratories, P. Pirouz of Case Western University, and E. Kvam of Liverpool University. The technical assistance of D. Bahnck is also gratefully acknowledged.

- <sup>1</sup>G. C. Osburn, IEEE J. Quantum Electron. **QE-22**, 1677 (1986).
- <sup>2</sup>J. C. Bean, in *Proceedings of the Materials Research Society*, edited by J. M. Gibson and L. R. Dawson (Materials Research Society, Pittsburgh, PA, 1985), Vol. 37, p. 245.
- <sup>3</sup>J. H. Van der Merwe and C. A. B. Ball, in *Epitaxial Growth*, edited by J. W. Matthews (Academic, New York, 1975), Pt. b, pp. 493-528.
- <sup>4</sup>J. W. Matthews and A. E. Blakeslee, J. Cryst. Growth **27**, 118 (1974); **32**, 265 (1974).
- <sup>5</sup>R. Hull, A. T. Fiory, J. C. Bean, J. M. Gibson, L. Scott, J. L. Benton, and S. Nakahara, in *Proceedings of the 13th International Conference on Defects in Semiconductors, Coronado, CA, 1984*, edited by L. C. Kimmerling and J. M. Parsey, Jr.

- (AIME, Warrendale, PA, 1985), p. 505.
- <sup>6</sup>A. T. Fiory, J. C. Bean, R. Hull, and S. Nakahara, Phys. Rev. B **31**, 4063 (1985).
- <sup>7</sup>B. W. Dodson and J. Y. Tsao, Appl. Phys. Lett. **51**, 1325 (1987).
- <sup>8</sup>J. Y. Tsao, B. W. Dodson, S. T. Picreux, and D. M. Cornelson, Phys. Rev. Lett. **59**, 2455 (1987).
- <sup>9</sup>H. Alexander and P. Haasen, Solid State Phys. **22**, 27 (1968).
- <sup>10</sup>R. Hull, J. C. Bean, D. J. Werder, and R. E. Leibenguth, Appl. Phys. Lett. **52**, 1605 (1988).
- <sup>11</sup>J. R. Patel and A. R. Chaudhuri, Phys. Rev. **143**, 601 (1966).
- <sup>12</sup>W. Hagen and H. Strunk, Appl. Phys. **17**, 85 (1978).
- <sup>13</sup>K. Rajan and M. Denhoff, J. Appl. Phys. **62**, 1710 (1987).

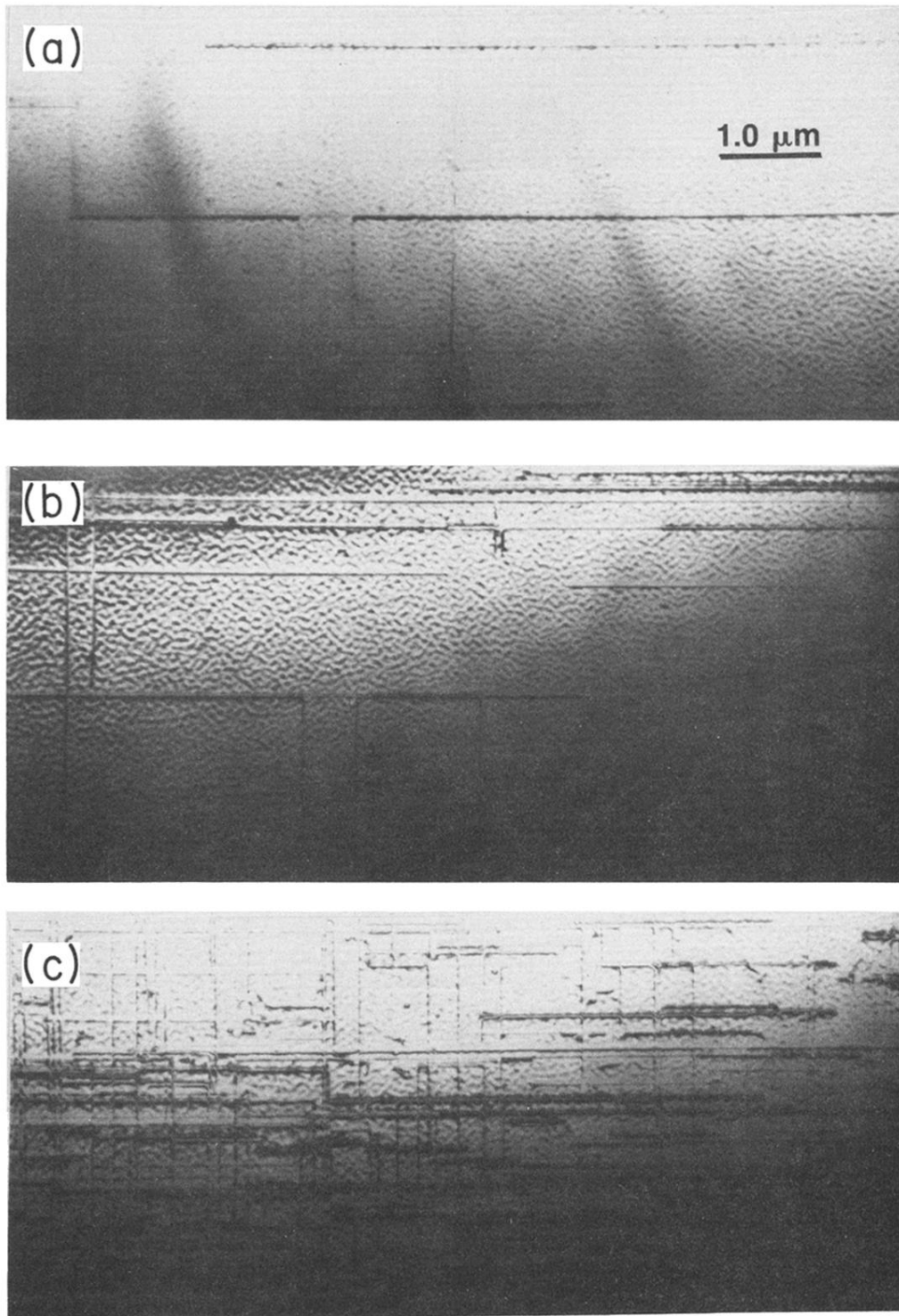


FIG. 1.  $\langle 022 \rangle$  plan-view TEM images of 350-Å  $\text{Ge}_{0.3}\text{Si}_{0.7}/\text{Si}(100)$  films: (a) as grown, and annealed for 4 min at (b) 700°C and (c) 900°C. Orthogonal arrays of  $\frac{1}{2}\langle 011 \rangle$  dislocations are observed.